Review Article | Pediatric Imaging

http://dx.doi.org/10.3348/kjr.2016.17.2.198
pISSN 1229-6929 · eISSN 2005-8330
Korean J Radiol 2016;17(2):198-208

Korean Journal of Radiology
KJR

Advances in Multidetector CT Diagnosis of Pediatric Pulmonary Thromboembolism

Paul G. Thacker, MD[1], Edward Y. Lee, MD, MPH[2]

[1]Department of Radiology and Radiological Science, Medical University of South Carolina, Charleston, SC 29425, USA; [2]Division of Thoracic Imaging, Department of Radiology and Medicine, Pulmonary Division Boston Children's Hospital, Harvard Medical School, Boston, MA 02115, USA

Although pediatric pulmonary thromboembolism is historically believed to be rare with relatively little information available in the medical literature regarding its imaging evaluation, it is more common than previously thought. Thus, it is imperative for radiologists to be aware of the most recent advances in its imaging information, particularly multidetector computed tomography (MDCT), the imaging modality of choice in the pediatric population. The overarching goal of this article is to review the most recent updates on MDCT diagnosis of pediatric pulmonary thromboembolism.

Index terms: *Pulmonary embolism; Dual-energy; Computed tomography*

INTRODUCTION

Pediatric pulmonary thromboembolism has historically been considered as rare with relatively little information present in the medical literature regarding its imaging evaluation. Buck et al. (1) have performed a retrospective review of 3600 pediatric autopsy patients and reported that the incidence of pulmonary thromboembolism is 3.7%. Additionally, they have found that massive pulmonary thromboembolism has contributed to death in 31% of cases. With increased use of advanced cross-section imaging, particularly computed tomography pulmonary angiography (CTPA), the prevalence of pediatric pulmonary thromboembolism has been found to be more common than previously thought. In recent articles by Kritsaneepaiboon et al. (2) and Victoria et al. (3), pulmonary thromboembolism prevalence in children who underwent CTPA for clinically suspected pulmonary thromboembolism ranged from 14% to 15.5%. Given these important findings, it is imperative for radiologist to be aware of the most recent advances in CT evaluation of pediatric pulmonary thromboembolism. In order to facilitate the understanding of pulmonary thromboembolism in the pediatric population, this article reviewed the underlying pathophysiology of pulmonary thromboembolism, clinical presentation, risk factors including recently published risk factor algorithm, CT techniques, imaging evaluation, the spectrum of imaging findings in both acute and chronic pulmonary embolism, and alternative diagnoses that may be seen for children who were clinically suspected of pulmonary thromboembolism but without the presence or findings of pulmonary thromboembolism.

Received July 23, 2015; accepted after revision December 18, 2015.

Corresponding author: Edward Y. Lee, MD, MPH, Division of Thoracic Imaging, Department of Radiology and Medicine, Pulmonary Division Boston Children's Hospital, Harvard Medical School, 300 Longwood Ave. Boston, MA 02115, USA.
• Tel: (1617) 355-3181 • Fax: (1617) 730-0635
• E-mail: Edward.Lee@childrens.harvard.edu

Pathophysiology

In adults, multiple studies have demonstrated that clot is most commonly originated from the lower extremity

Korean Journal of Radiology
KJR

venous valve pockets. However, in the pediatric population, the upper extremity veins play more prominent roles (4-9). Unlike adults where pulmonary thromboembolism is idiopathic in nearly one-third of patients, children with pulmonary thromboembolism have an identifiable risk factor in 96–98% of cases (10, 11). Given the high prevalence of risk factors in the pediatric population, d-dimer measurement is less reliable. Therefore, it is not routinely used as it is often elevated by underlying risk factors regardless of the presence or absence of pulmonary thromboembolism (10, 12, 13).

Once pulmonary thromboembolism is developed, its physiological effects are dependent on vasoactive mediator presence, the amount of pulmonary circulation obstructed, and the concomitant cardiopulmonary disease. Pulmonary thromboembolism obstructing < 50% of pulmonary circulation are often clinically silent without underlying cardiopulmonary disease (10, 12). When pulmonary circulation involvement exceeds 50%, significant increases in the right ventricular afterload will occur, leading to right ventricular dilatation, increased pulmonary arterial pressure, and higher right ventricular pressure (10). In cases of pulmonary arterial hypertension, the left main coronary artery is compressed by the enlarged main pulmonary artery, resulting in cardiac ischemia and ultimately leading to hypotension due to diminished cardiac output (10).

Clinical Presentation

The classic PE presentation of hemoptysis, shortness of breath, and pleuritic chest pain is often not seen in children unless a large amount of pulmonary thromboembolism is present (10, 14, 15). Thus, pediatric pulmonary thromboembolism often presents with subtle and vague symptoms that can mimic other pulmonary diseases. Children often have excellent cardiac reserve to help them compensate for a large pulmonary thromboembolism burden. Thus, a high clinical suspicion is vital. Affected older children most commonly (84% of cases) present with pleuritic chest pain (16). Pediatric patients may also present with dysrhythmia, syncope, unexplained tachypnea, hypotension, and right heart failure. Of note, tachypnea is an important indicator of pulmonary thromboembolism in all pediatric patients (10, 17).

Risk Stratification Algorithm

Well-defined and widely utilized algorithms have been established to manage pulmonary embolism for adults. However, pediatric pulmonary thromboembolism prediction algorithms are just now coming to light. In a recent study for 227 CTPA performed in 227 patients who are clinically suspected of having pulmonary thromboembolism, the following five statistically significant risk factors for pulmonary thromboembolism have been found: immobilization, hypercoagulable state, excess estrogen state, indwelling central venous catheters (CVC), and prior pulmonary thromboembolism and/or deep venous thrombosis (Table 1) (18). Of 36 patients who were positive for pulmonary emboli, 37% were located in segmental pulmonary arteries, 31% were in lobar pulmonary arteries, 23% were in subsegmental pulmonary arteries, and 9% were in main or central pulmonary arteries. In patients with pulmonary thromboembolism, immobilization (75%) was the most common risk factor, followed by CVC (56%), prior pulmonary emboli and/or deep venous thrombosis (44%), hypercoagulable state (22%), and excess estrogen state, i.e., oral contraceptive usage (22%). Two of 36 patients were found to have pulmonary thromboembolism on CTPA without identifiable risk factors. Conversely, of 191 pediatric patients who were found not to have pulmonary thromboembolism on CTPA, no risk factor was found in 121 patients (63%). In those patients who were negative for pulmonary thromboembolism, 59 (31%) had one risk factor while 11 (6%) had two risk factors. None of the patients without pulmonary thromboembolism had

Table 1. Significant Independent Risk Factors for Pulmonary Thromboembolism

Risk Factor	β Coefficient	Odds Ratio	95% CI	*P*
Immobilization	4.87	130.5	25.0, 681.8	< 0.001
Hypercoagulable state	3.06	21.4	3.5, 131.5	0.003
Excess estrogen state	2.58	13.2	1.5, 123.7	0.002
Indwelling CVL	3.28	26.4	5.5, 127.2	< 0.001
Prior PE and/or DVT	1.96	7.1	2.0, 27.2	< 0.001

Reprinted from Lee et al. *Radiology* 2012;262:242-251, with permission of Radiological Society of North America (18). CI = confidence interval, CVL = central venous line, DVT = deep venous thrombosis, PE = pulmonary thromboembolism

greater than two risk factors. The authors were able to calculate the probability of pulmonary thromboembolism based on the number of risk factors present (Table 2). In the absence of any risk factor, the probability of pulmonary thromboembolism was found to be 0.5%. With one risk factor, the probability was 8%. Pulmonary thromboembolism probability with two and three or more risk factors was 62% and 89%, respectively. With two or more of these risk factors as clinical threshold, the sensitivity and specificity for a positive pulmonary thromboembolism were 89% and 94%, respectively. Thus, the authors concluded that clinical assessment for these five risk factors should be employed as a first-line triage method to determine the necessity of imaging evaluation (Fig. 1) (18). Of note, in that study, the authors found no significant difference in age or sex of patients with pulmonary thromboembolism compared to those who did not have pulmonary thromboembolism. However, in neonates, CVC with associated thrombus has been found in 80% of cases (10, 14, 19). After the neonatal period, the single greatest risk factor is the presence of a CVC. However, additional risk factors begin to have increasing roles.

CT Technique

Patient Preparation

To perform CTPA, patient preparation is primarily based on whether sedation is required and what size intravenous catheter is utilized. For patients ≥ 5 years of age who can follow breathing instructions, sedation is generally not required. By contrast, infants and children less than 5 years old are generally sedated for CTPA. Since newer generation scanners have the capability of scanning the entire chest with sub-second scan times, sedation is less likely to be utilized. At our institutions, CTPA studies are performed with nonionic contrast at a dose of 2 mL/kg (not to exceed 4 mL/kg or 125 mL). Contrast may be injected either manually or by power injection if the patient has a secure antecubital catheter. Power injection rates are 3 mL/s for a 20-gauge catheter, 1.5–2.0 mL/s for a 22-gauge catheter, and 1.0 mL/s for a 24-gauge catheter. If the catheter is placed in the hand or foot, manual injection is generally performed with an injection rate of approximate 1 mL/s. Contrast administration should be closely monitored during the initial injection to minimize contrast extravasation risk (2).

Table 2. Simplified Algorithm of Number of Risk Factors and Probability of Pulmonary Thromboembolism

No. of Risk Factors*	Probability of PE (%)	95% CI (%)
None	0.5	0.1, 2
Any one	8	5, 15
Any two	62	46, 76
Any three or more	89	87, 99

Reprinted from Lee et al. *Radiology* 2012;262:242-251, with permission of Radiological Society of North America (18). *Risk factors include immobilization, hypercoagulable state, excess estrogen state, indwelling central venous catheter, and prior pulmonary embolism and/or deep venous thrombosis. CI = confidence interval, PE = pulmonary embolism

CT Parameters

Patients are placed in supine position with an initial scout radiographic image acquired to define scan coverage so that the entirety of both lungs and from the level of the thoracic inlet to the diaphragms are covered. Scanning direction can be either craniocaudal or caudocranial. Acquiring images in the caudal-cranial direction may be useful given the higher prevalence of pulmonary embolism in the lower lobes. By acquiring images of the lower lobes first, one can reduce the chance that emboli may be obscured by respiratory motion in a patient who cannot hold their breath for the entire examination (2, 20). Kilovoltage and tube current

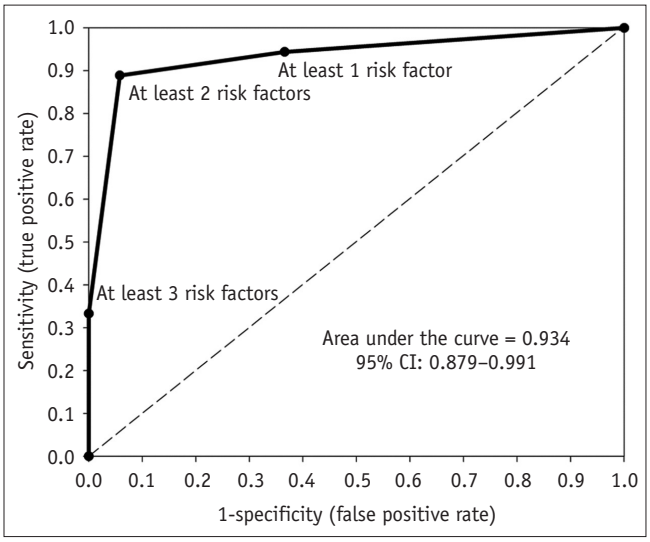

Fig. 1. Receiver operative characteristic curve for differentiating patients with pulmonary thromboembolism from those without pulmonary thromboembolism based on total number of risk factors (immobilization, indwelling central venous line, prior pulmonary thromboembolism and/or deep venous thrombosis, hypercoagulable state, and excess estrogen state). Dashed line = 45° line of nondiscrimination (equivalent to coin tossing). Area under curve of 0.934 indicates excellent discrimination (p = 0.0001). Reproduced from Lee et al. *Radiology* 2012;262:242-251, with permission of Radiology Society of North America (18). CI = confidence interval

Korean Journal of Radiology
KJR

can be adjusted based on the patient's size by closely following the as low as reasonably achievable principle. Based on patient size, specific techniques can be used, including manual tube current technique charts, automatic exposure control, size-dependent beam-shaping filters, and optimal tube potential (21). Lower kilovoltage scanning has been shown to increase the percentage of peripheral and central pulmonary arteries which can be evaluated while decreasing radiation dosage without substantially affecting image quality (22). In addition, employing currently available dose modulation techniques can further decrease the overall radiation dose when performing CTPA in children (2, 23-26).

Timing of Bolus

Two primary methods are used for bolus timing, i.e., bolus tracking and empiric scan delay. Test bolus administration is less often performed in pediatric population. Bolus tracking involves placing a region of interest over the pulmonary outflow tract or main pulmonary artery by either preselecting a desired threshold for the scan to start or visually monitoring and manually triggering the scan. After contrast material injection, a series of low-dose dynamic images are acquired for the region of interest. Once the desired Hounsfield units (HU), generally between 150 and 200 HU, are reached within the region of interest, a full diagnostic scan is then triggered. This method is advantageous as it allows for the tailoring of scan times in real-time for the particular cardiovascular physiology of patients. However, this advantage is counterbalanced with the possibility that the enhancement threshold will never be reached, thus creating an uncertainty for the technologist on when to start the scan (20). Additionally, some authors have argued that bolus tracking can result in less optimal pulmonary arterial enhancement compared to the empiric scan delay technique (20), although this has not been definitively demonstrated.

The empiric scan delay technique uses a preset time delay from the end of the contrast bolus to the beginning of the scan, generally ranging from 15 seconds to 25 seconds. This simple technique adds uniformity across scans, reducing the complexity involved and the potential operator error. Therefore, it has been suggested as the technique of choice for adult CTPA (20). However, these advantages are less certain in children given the wide variances in pediatric sizes and heart rates. It is our opinion that generally the empiric delay technique is more likely to lead to suboptimal vascular enhancement in comparison to bolus tracking in the pediatric population. Thus, we advocate bolus timing based on the bolus tracking method with preset attenuation thresholds or by manual triggering the scan.

Pulmonary arterial enhancement has also been shown to be affected by respiratory cycle, i.e., full inspiration, expiration, normal breathing, and free-breathing (27-30). It has been hypothesized that during full inspiration, contrast agent is diluted by differential flow rates in the inferior vena cava versus the superior vena cava. Additionally, patients may undergo a Valsalva maneuver in full inspiration that has been shown to be able to decrease pulmonary blood flow (27). Given these hemodynamic effects, shallow

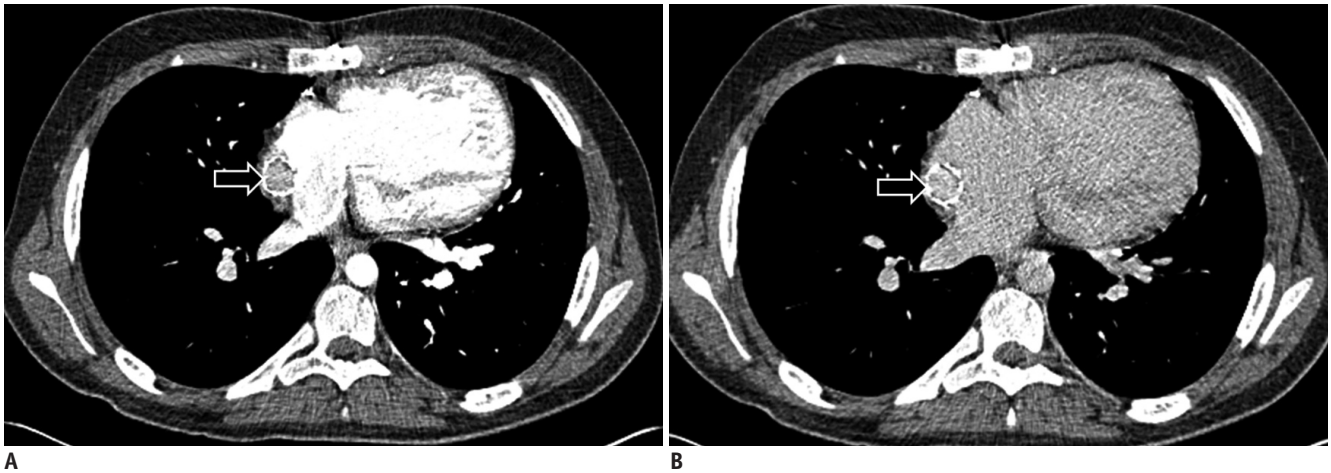

A B

Fig. 2. 16-year-old boy with history of double outlet right ventricle status post Fontan procedure who presented with shortness of breath.

A. Initial axial enhanced computed tomographic image showing low attenuation area (arrow) within Fontan pathway concerning for possible thrombosis. **B.** Subsequently obtained delayed axial computed tomographic image demonstrating homogeneous opacification of Fontan pathway (arrow) similar to other cardiovascular structures, confirming absence of thrombosis.

free-breathing and expiratory phase scanning have been advocated to overcome insufficient pulmonary arterial enhancement (27, 30).

One clinical circumstance that is worthy of specific consideration is the assessment of pulmonary thromboembolism in children who have undergone Fontan procedure for congenital heart disease. In these patients, contrast enhancement of the pulmonary arteries is often suboptimal due to the slow-moving blood flow through the Fontan pathway and the lack of contrast material mixing

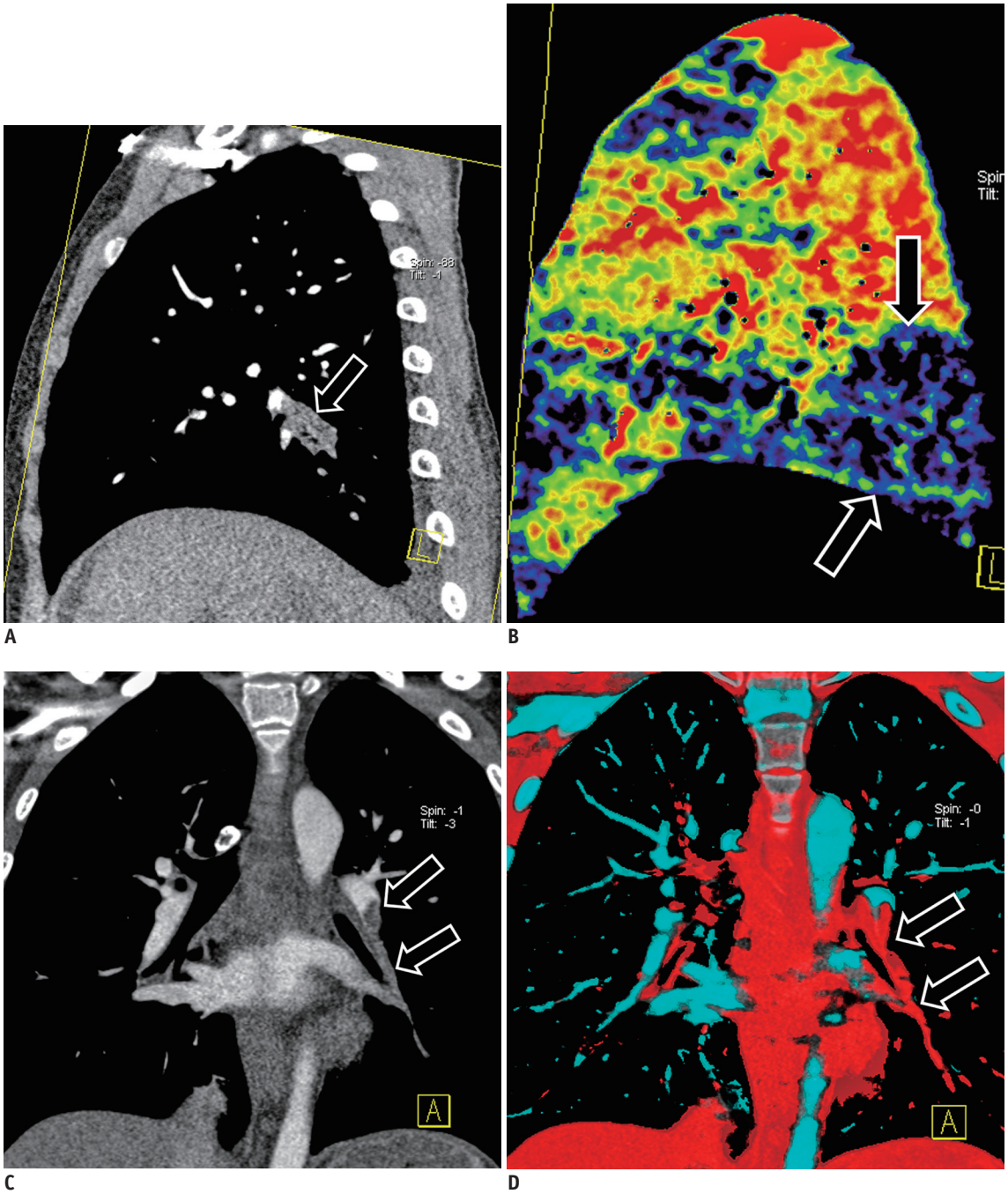

Fig. 3. Acute pulmonary embolism on dual-energy computed tomography.
A. Sagittal reformatted image demonstrating occlusive pulmonary embolism (arrow) in posterior basal branch of right pulmonary artery. **B.** Dual-energy computed tomography blood pool map demonstrating corresponding wedge-shaped area of decreased perfusion (arrows) in posterior basal right lower lobe. **C.** Coronal reformatted image from contrast-enhanced dual-energy computed tomography demonstrating occlusive thrombus (arrows) in left lower lobe pulmonary artery. **D.** Corresponding tissue-specific thrombus analysis demonstrating thrombus as red filling defect (arrows) with blue-shaped pulmonary artery. Images provided by courtesy of Dr. Long Jiang Zhang, Department of Medical Imaging, Jinling Hospital, Clinical School of Medical College, Nanjing University, China.

Korean Journal of Radiology
KJR

within the right atrium (Fig. 2). Due to the suboptimal contrast within the pulmonary arteries, evaluation for pulmonary thromboembolism can be incomplete, which can lead to misdiagnosis of pulmonary thromboembolism when no thromboembolism is present (31). In a recent case series, Prabhu et al. (31) described their experience in evaluating 5 pediatric patients who had Fontan procedure and multidetector CT (MDCT) for suspected pulmonary thromboembolism. Three of the patients were initially misdiagnosed as having pulmonary thromboembolism due to suboptimal contrast-enhancement technique using a single injection of contrast material through an upper extremity vein. They described the following three technical parameters that could be used to optimize CTPA in those patients with a Fontan: simultaneous injection of contrast material through lower- and upper-extremity veins, the usage of a delayed second-phase scan if there is a suboptimal contrast enhancement on the initial images or in patients with bilateral Glenn shunts with sluggish blood flow in the Fontan circulation or in the pulmonary arteries (Fig. 2), and employing bolus tracking with optimal contrast enhancement within the Fontan pathway and the pulmonary arteries (31). Alternatively, an additional useful technique for assessing Fontan pathway thromboembolism is to give patient a single intravenous injection of the leg at a slow injection rate with a single delay-phase scan at 1–3 minutes (32).

Dual-Energy CT

Dual-energy CT (DECT) represents a recent technical innovation in CT imaging. It allows for both anatomic and functional lung imaging in a single test (33). Images are acquired by scanning the chest with two different X-ray spectra to allow the differentiation of materials of different densities based on Compton scatter and electric absorption (34). In the chest, a combination of 80 kVp and 140 kVp energy spectra are generally employed with radiation dose similar to that of single-energy CT (34, 35). Images are most often acquired during full inspiration, although imaging with free-breathing has been described (33). Once the initial dataset is acquired, images are post-processed using three-material decomposition by differentiating body tissues from lung contrast agents, e.g., iodinated intravenous contrast in CT perfusion and xenon in CT ventilation imaging (34). In CT perfusion imaging, pulmonary vessels can be divided into enhanced and unenhanced vessels based on local iodine values. Given this ability, one major emerging clinical application for DECT is to evaluate pediatric pulmonary thromboembolism (Fig. 3). In animal models, CT perfusion imaging has been shown to increase the sensitivity of detecting peripheral pulmonary thromboembolism (36). With the addition of CT ventilation imaging, ventilation/perfusion mismatches may be seen, thus increasing the confidence in PE diagnosis. Although multiple studies have demonstrated the feasibility of this technique for adults, its experience in children remains limited. However, with more widespread usage of dual-energy technique, DECT, particular perfusion imaging, could become the standard technique for pulmonary thromboembolism imaging.

Imaging Evaluation

Axial CT Evaluation

Axial CT images are generally the first ones reviewed from any chest CT images to determine pulmonary thromboembolism. They should be evaluated with soft tissue (window [W] = 350, level [L] = 50), lung (W = 1500, L = -500), and vascular windows (W = 700, L = 200). Evaluation can begin by starting at the level of the main pulmonary arteries and working distally within each branch of the pulmonary arteries until the artery can no longer be identified. Alternatively, one can start from either the top or the bottom of the scanning area and evaluate each arterial branch by working proximally towards the main pulmonary artery. Diagnosis is made by the demonstration of direct or indirect findings of acute or chronic pulmonary embolus (discussed below) on two or more consecutive axial sequences. When pulmonary thromboembolism is identified, the pulmonary artery level involved (e.g., central, lobar, segmental or subsegmental), the affect lobe, and any associated parenchymal changes should be documented. After studying 84 children who underwent 98 CTPAs for pulmonary thromboembolism, Kritsaneepaiboon et al. (2) have found that pulmonary emboli located in lobar pulmonary arteries occurred in 39% of cases, segmental pulmonary arteries in 35% of patients, subsegmental pulmonary arteries in 16% of cases, and main or central pulmonary arteries in 10% of patients. Right lower lobe was found in 37% of cases, which was the most common one. Left lower lobe was the next most common (24%), followed by right upper lobe in 15% of cases, and the right middle lobe or the left upper lobe (12% of cases each) (2). Pulmonary thromboembolism was most often bilateral (61%)

or multilobar (46%). When pulmonary thromboembolism is unilateral, the right lung is often affected (2).

Multiplanar Reformatted CT Image Evaluation

Following acquisition of the initial CT data set, multiplanar reformations (MPR) are often generated with most institutions routinely generating coronal images (Fig. 4). Depending on institutional preferences, sagittal and oblique planes may also be created. These added planes can significantly increase confidence and interobservor agreement for pulmonary thromboembolism diagnosis as demonstrated in a study by Lee et al. (25) after retrospectively reviewing 60 children who underwent CTPA for clinically suspected pulmonary thromboembolism. They found a diagnostic accuracy of CTPA for pulmonary thromboembolism ranging from 91.7% to 100% with a mean of 96.7%. In addition, there was no significant difference between axial images and MPR MDCT images. However, they found that the use of MPR images significantly increased the interpretation times and interobservor agreement. Thus, additional MPR images may be usefulness for cases whose diagnosis of pulmonary thromboembolism is in question (25). Extrapolating from their data, one could evaluate axial images first. If the diagnosis of pulmonary thromboembolism is firmly confirmed or excluded, no additional reformation is need. However, if after reviewing the axial images, the diagnosis is in question, additional MPR images can then be generated. This approach might balance accuracy, time efficiency, and reader confidence.

Spectrum of Imaging Findings

The criteria for pulmonary thromboembolism diagnosis can be divided based on chronicity (i.e., acute versus chronic) and further subdivided based on direct or indirect signs of pulmonary thromboembolism.

Acute Pulmonary Thromboembolism Signs

Direct Signs

Direct signs of acute pulmonary thromboembolism have been well documented throughout the medical literature. They are the same regardless of patient age. The most definitive sign is complete arterial occlusion (Fig. 5). In this case, there is a failure to completely opacify the arterial lumen with the embolus measured at less HU than the adjacent opacified blood (20, 37). The affected pulmonary artery may be enlarged compared to pulmonary

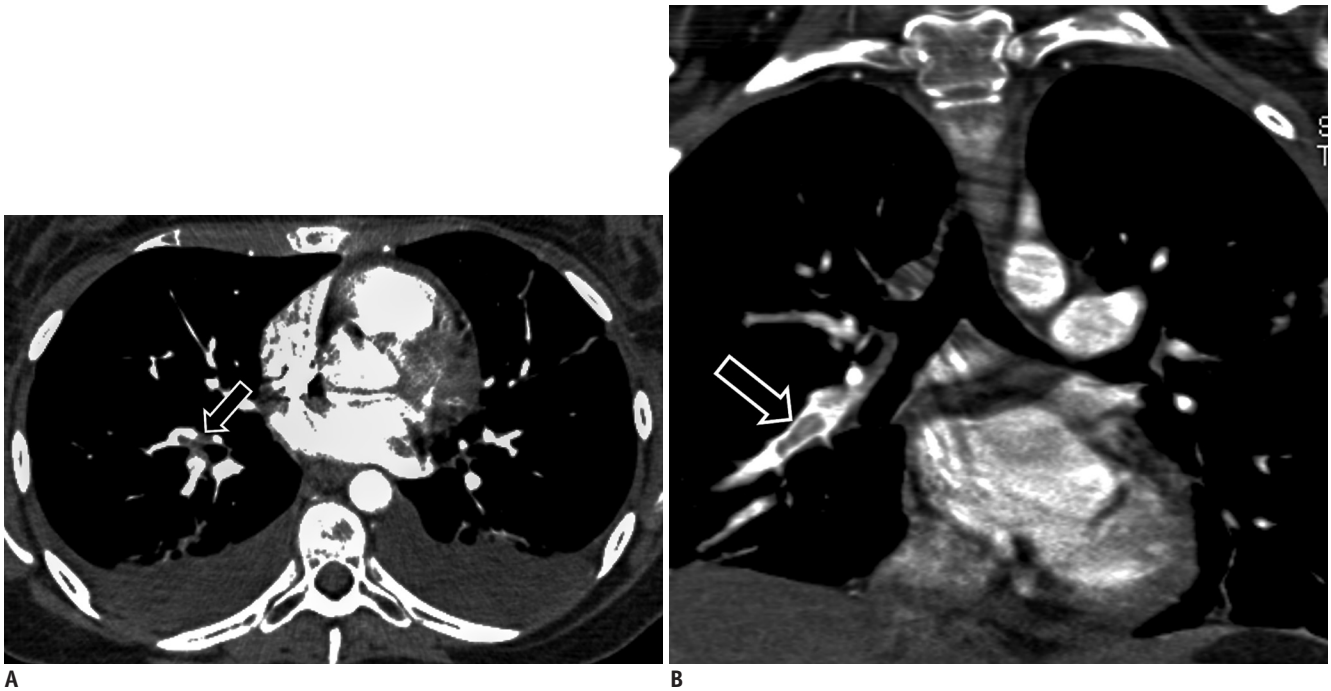

A B

Fig. 4. 15-year-old girl with oral contraceptive medication who presented with acute shortness of breath and chest pain.
A. Axial enhanced computed tomographic image showing low attenuation area (arrow) near right lower lobe pulmonary arteries. It was initially interpreted as lymph nodes based on axial computed tomographic image alone. Also noted are bilateral pleural effusions. **B.** Coronal enhanced computed tomographic image demonstrating intraluminal filling defect (arrow) in right lower lobe pulmonary artery, confirming diagnosis of pulmonary embolism which was initially overlooked based on axial computed tomographic image alone **(A)**.

Korean Journal of Radiology
KJR

arteries with the same branching order (20). Alternatively, if the embolus is not completely occlusive, it may appear as a central filling defect surrounded by intravenous contrast material (Fig. 4B). A third direct sign of acute pulmonary thromboembolism is that a peripheral intraluminal defect can form an acute angle with the vessel wall. Any of these three direct signs can be present on two or more contiguous slices (2, 20).

Indirect Signs

Indirect signs of acute pulmonary thromboembolism are divided into indirect vascular signs and lung parenchymal changes. Indirect vascular signs include nonuniform arterial perfusion and oligemia corresponding to the classic Westermark sign on chest radiography. These findings are more often seen in cases of severe pulmonary thromboembolism. It is difficult to recognize them on chest CT. Nevertheless, these findings are more readily apparent on CT compared to chest radiography. Occasionally, nonuniform arterial perfusion manifests as mosaic pattern of lung attenuation on lung windows (Fig. 6). However, this findings is more commonly seen in chronic pulmonary thromboembolism (20).

By contrast, lung parenchymal changes are readily demonstrable, including wedge-shaped peripheral consolidation, linear opacities, pleural effusions, ground-glass opacities, atelectasis, nodules, and focal patchy increased attenuation (Fig. 7). On review of the above list of parenchymal changes, it is apparent that most of these findings are nonspecific with a rather long differential diagnosis. However, after evaluating lung parenchymal and pleural abnormalities in children with or without pulmonary thromboembolism, Lee et al. (26) found that wedge-shaped areas of consolidation were significantly more common in children with pulmonary thromboembolism than in those without pulmonary thromboembolism (36% of children with pulmonary thromboembolism and 9% of children without pulmonary thromboembolism, $p = 0.03$). Nevertheless, indirect signs of acute pulmonary thromboembolism other than wedge-shaped consolidations have limited usefulness. They might help direct the interpreting radiologist to carefully look for direct signs of pulmonary thromboembolism in the involved area.

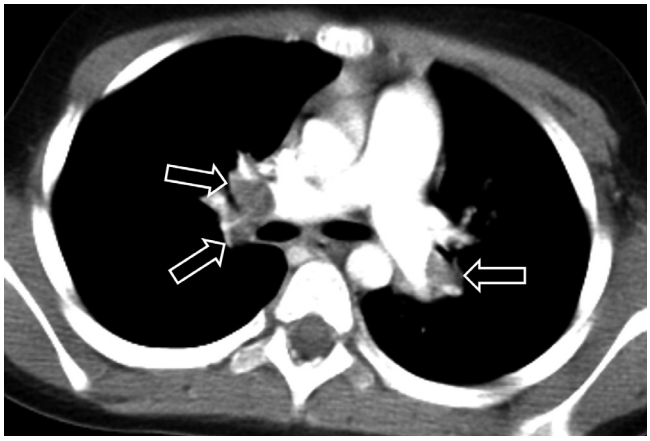

Fig. 5. 4-year-old girl with neuroblastoma who presented with shortness of breath and chest pain. Axial enhanced computed tomographic image showing bilateral pulmonary embolism (arrows).

Chronic Pulmonary Thromboembolism Signs

Direct Signs

Direct signs of chronic pulmonary thromboembolism have a more varied morphology in comparison to acute pulmonary thromboembolism direct signs. Chronic pulmonary thromboembolism may appear as intraluminal filling defect present for more than 3 months with acute pulmonary thromboembolism morphology. Alternatively, the vessels may be completely occluded and permanently shrunken compared to its neighboring vessels. An eccentric filling defect forming an obtuse margin with the vessel wall

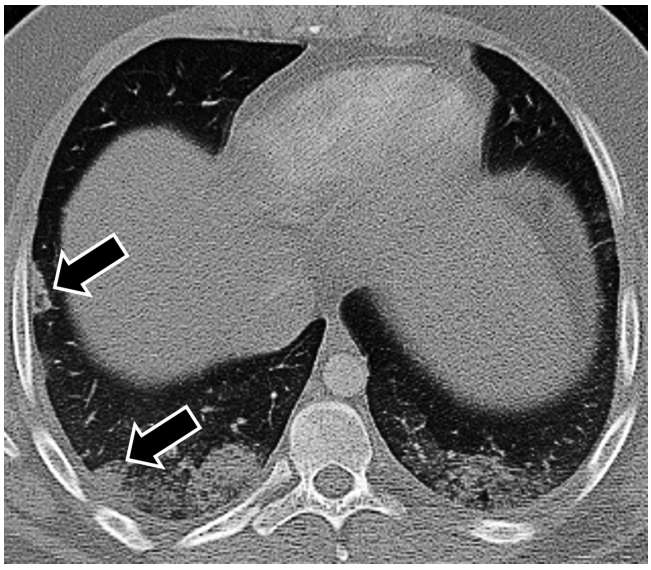

Fig. 6. 17-year-old African-American male with recent history of immobilization after motor vehicle collision and acute onset of tachycardia. Axial contrast-enhanced chest computed tomographic image through lower lobe demonstrating small bilateral pleural effusions and peripheral opacities, some of which are wedge-shaped (arrows), consistent with parenchymal changes of pulmonary emboli (not shown on this). Additionally, there is subtle mosaic attenuation of lungs with lower lobes more opacified in respect to partially visualized right middle lobe and lingula, subtle indirect finding of pulmonary emboli due to nonuniform perfusion.

(Fig. 8) may be seen (20). Additional direct signs include intraluminal web or band within an otherwise contrast-opacified artery and apparent thick-walled artery with contrast passing through irregular lumen representing recanalization within chronic thrombus (20). Occasionally, chronic pulmonary emboli may be calcified.

Indirect Signs

Much like indirect signs of acute pulmonary thromboembolism that mostly serve as a harbinger of pulmonary thromboembolism and direct the radiologist to areas for closer scrutiny, indirect signs of chronic pulmonary thromboembolism are also largely nonspecific. As mentioned above, mosaic attenuation of lungs is more commonly seen in chronic rather than acute pulmonary thromboembolism as a manifestation of non-uniform arterial perfusion (20). Other indirect signs of chronic pulmonary thromboembolism include enlargement of the bronchial arteries, tortuous pulmonary vessels, poststenotic arterial dilatation, and abrupt cutoff of a pulmonary artery or peripheral pruning (20, 38). Signs of pulmonary hypertension with right heart enlargement and pulmonary arterial enlargement may be present.

CT Perfusion Findings

In addition to the direct and indirect signs of pulmonary thromboembolism demonstrated on standard axial CT images, lung perfusion defects or abnormalities can be seen on axial overlaid DECT images (Fig. 3). Here, perfusion abnormalities are dependent on the overall thrombotic burden and the site as well as the extent of vessel occlusion. In general, occlusive thrombi demonstrate focal or regional perfusion defects that have been shown to correlate well with the lack of lung perfusion on other imaging modalities (33, 34, 39-42).

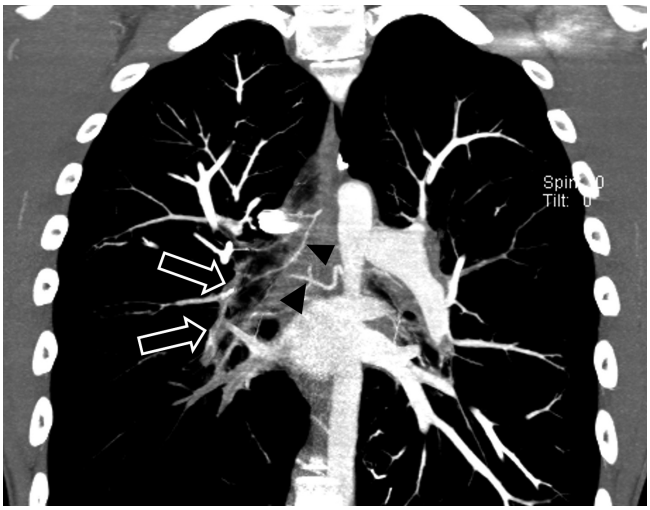

Fig. 8. 16-year-old girl with oral contraceptive medication and chronic pulmonary embolism. Coronal maximum intensity projection computed tomographic image showing eccentric filling defects (arrows) which form obtuse margin with vessel wall. Also noted are several prominent enlarged bronchial arteries (arrowheads) coursing along pulmonary arteries containing chronic pulmonary embolism.

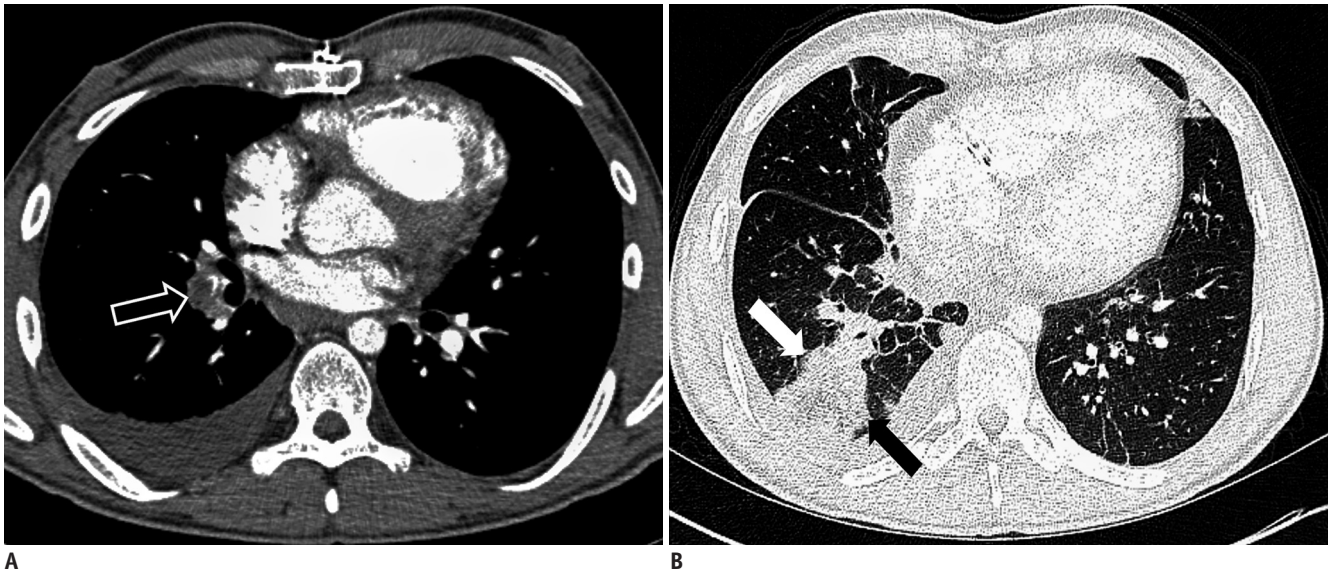

A B

Fig. 7. 15-year-old girl with repaired congenital heart disease who presented with acute right sided chest pain.
A. Axial enhanced computed tomographic image showing filling defect (arrow) in right lower lobe segmental pulmonary artery. Also noted is right pleural effusion. **B.** Axial lung window computed tomographic showing wedge shaped (arrows) opacity consistent with lung infarction from pulmonary embolism.

Korean Journal of Radiology
KJR

Alternative Diagnoses

Similar to adults where significant alternative diagnosis has been made for majority of patients who are clinically suspected of pulmonary thromboembolism, over half of children suspected of having pulmonary thromboembolism do not have pulmonary emboli or an alternative diagnosis discovered at CT (24). Thus, it is imperative for the interpreting radiologist to be aware of these alternative diagnoses before interpreting CTPA for pediatric pulmonary thromboembolism. In a recent study, of 89 children with age ranging from 2 months to 18 years who underwent 96 CTPAs but found not to have pulmonary thromboembolism, 59% of patients are found to have alternative diagnosis (24). The most common alternative diagnoses are pneumonia and atelectasis. One of these two diagnoses were found in 77% (44/57) of patients, including atelectasis in 22 patients and pneumonia in 22 patients. The next most common alternative diagnosis is malignancy (5%). Congenital heart disease, pulmonary hypertension, and pericardial effusion are each found in 3.5% of cases. Lastly, pulmonary nodules, rib fractures, right atrial thrombus, and fat embolism are each found in 1.8% of cases (24). These findings buoy the fact that a systematic search beyond pulmonary arteries is warranted in all MDCT for pediatric pulmonary thromboembolism.

CONCLUSION

Once thought to be rare, recent research studies have demonstrated that pediatric pulmonary thromboembolism has a higher prevalence than previously thought. Historically, lung ventilation-perfusion scintigraphy (VQ scan) has served as the first-line modality to detect pediatric pulmonary thromboembolism. However, CT is currently the imaging modality of choice with VQ scans primarily serving secondarily as a problem solving tool. Although imaging interpretation for pediatric pulmonary thromboembolism is similar to that for adults, awareness of alternative diagnosis as well as up-to-date low dose CT techniques, particularly DECT lung perfusion imaging, is imperative for optimal scan quality and interpretation (43). Furthermore, recently described and future risk stratification algorithms will likely begin to be routinely incorporated into clinical practice. This could potentially decrease pediatric radiation exposure by only performing CT in those at high risk of pulmonary thromboembolism.

REFERENCES

1. Buck JR, Connors RH, Coon WW, Weintraub WH, Wesley JR, Coran AG. Pulmonary embolism in children. *J Pediatr Surg* 1981;16:385-391
2. Kritsaneepaiboon S, Lee EY, Zurakowski D, Strauss KJ, Boiselle PM. MDCT pulmonary angiography evaluation of pulmonary embolism in children. *AJR Am J Roentgenol* 2009;192:1246-1252
3. Victoria T, Mong A, Altes T, Jawad AF, Hernandez A, Gonzalez L, et al. Evaluation of pulmonary embolism in a pediatric population with high clinical suspicion. *Pediatr Radiol* 2009;39:35-41
4. Browse NL, Thomas ML. Source of non-lethal pulmonary emboli. *Lancet* 1974;1:258-259
5. Rollins DL, Semrow CM, Friedell ML, Lloyd WE, Buchbinder D. Origin of deep vein thrombi in an ambulatory population. *Am J Surg* 1988;156:122-125
6. Howe CT, Kakkar VV, Flanc C, Clarke MB. The natural history of deep-vein thrombosis. *Br J Surg* 1969;56:625
7. Kakkar VV, Howe CT, Flanc C, Clarke MB. Natural history of postoperative deep-vein thrombosis. *Lancet* 1969;2:230-232
8. Nicolaides AN, Kakkar VV, Renney JT. The soleal sinuses: origin of deep-vein thrombosis. *Br J Surg* 1970;57:860
9. Nicolaides AN, Kakkar VV, Field ES, Renney JT. The origin of deep vein thrombosis: a venographic study. *Br J Radiol* 1971;44:653-663
10. Patocka C, Nemeth J. Pulmonary embolism in pediatrics. *J Emerg Med* 2012;42:105-116
11. Andrew M, David M, Adams M, Ali K, Anderson R, Barnard D, et al. Venous thromboembolic complications (VTE) in children: first analyses of the Canadian Registry of VTE. *Blood* 1994;83:1251-1257
12. Van Ommen CH, Peters M. Acute pulmonary embolism in childhood. *Thromb Res* 2006;118:13-25
13. Kelly J, Rudd A, Lewis RR, Hunt BJ. Plasma D-dimers in the diagnosis of venous thromboembolism. *Arch Intern Med* 2002;162:747-756
14. van Ommen CH, Heijboer H, Büller HR, Hirasing RA, Heijmans HS, Peters M. Venous thromboembolism in childhood: a prospective two-year registry in The Netherlands. *J Pediatr* 2001;139:676-681
15. Chan AK, Deveber G, Monagle P, Brooker LA, Massicotte PM. Venous thrombosis in children. *J Thromb Haemost* 2003;1:1443-1455
16. Bernstein D, Coupey S, Schonberg SK. Pulmonary embolism in adolescents. *Am J Dis Child* 1986;140:667-671
17. van Ommen CH, Heyboer H, Groothoff JW, Teeuw R, Aronson DC, Peters M. Persistent tachypnea in children: keep pulmonary embolism in mind. *J Pediatr Hematol Oncol* 1998;20:570-573
18. Lee EY, Tse SK, Zurakowski D, Johnson VM, Lee NJ, Tracy DA, et al. Children suspected of having pulmonary embolism: multidetector CT pulmonary angiography--thromboembolic

risk factors and implications for appropriate use. *Radiology* 2012;262:242-251
19. Schmidt B, Andrew M. Neonatal thrombosis: report of a prospective Canadian and international registry. *Pediatrics* 1995;96(5 Pt 1):939-943
20. Wittram C. How I do it: CT pulmonary angiography. *AJR Am J Roentgenol* 2007;188:1255-1261
21. Yu L, Bruesewitz MR, Thomas KB, Fletcher JG, Kofler JM, McCollough CH. Optimal tube potential for radiation dose reduction in pediatric CT: principles, clinical implementations, and pitfalls. *Radiographics* 2011;31:835-848
22. Schueller-Weidekamm C, Schaefer-Prokop CM, Weber M, Herold CJ, Prokop M. CT angiography of pulmonary arteries to detect pulmonary embolism: improvement of vascular enhancement with low kilovoltage settings. *Radiology* 2006;241:899-907
23. Lee CH, Goo JM, Ye HJ, Ye SJ, Park CM, Chun EJ, et al. Radiation dose modulation techniques in the multidetector CT era: from basics to practice. *Radiographics* 2008;28:1451-1459
24. Lee EY, Kritsaneepaiboon S, Zurakowski D, Arellano CM, Strauss KJ, Boiselle PM. Beyond the pulmonary arteries: alternative diagnoses in children with MDCT pulmonary angiography negative for pulmonary embolism. *AJR Am J Roentgenol* 2009;193:888-894
25. Lee EY, Zucker EJ, Tsai J, Tracy DA, Cleveland RH, Zurakowski D, et al. Pulmonary MDCT angiography: value of multiplanar reformatted images in detecting pulmonary embolism in children. *AJR Am J Roentgenol* 2011;197:1460-1465
26. Lee EY, Zurakowski D, Diperna S, d'Almeida Bastos M, Strauss KJ, Boiselle PM. Parenchymal and pleural abnormalities in children with and without pulmonary embolism at MDCT pulmonary angiography. *Pediatr Radiol* 2010;40:173-181
27. Renne J, Falck Cv, Ringe KI, Raatschen HJ, Wacker F, Shin HO. CT angiography for pulmonary embolism detection: the effect of breathing on pulmonary artery enhancement using a 64-row detector system. *Acta Radiol* 2014;55:932-937
28. Kuzo RS, Pooley RA, Crook JE, Heckman MG, Gerber TC. Measurement of caval blood flow with MRI during respiratory maneuvers: implications for vascular contrast opacification on pulmonary CT angiographic studies. *AJR Am J Roentgenol* 2007;188:839-842
29. Mortimer AM, Singh RK, Hughes J, Greenwood R, Hamilton MC. Use of expiratory CT pulmonary angiography to reduce inspiration and breath-hold associated artefact: contrast dynamics and implications for scan protocol. *Clin Radiol* 2011;66:1159-1166
30. Chen YH, Velayudhan V, Weltman DI, Balsam D, Patel N, Draves KA, et al. Waiting to exhale: salvaging the nondiagnostic CT pulmonary angiogram by using expiratory imaging to improve contrast dynamics. *Emerg Radiol* 2008;15:161-169
31. Prabhu SP, Mahmood S, Sena L, Lee EY. MDCT evaluation of pulmonary embolism in children and young adults following a lateral tunnel Fontan procedure: optimizing contrast-enhancement techniques. *Pediatr Radiol* 2009;39:938-944
32. Han BK, Lesser JR. CT imaging in congenital heart disease: an approach to imaging and interpreting complex lesions after surgical intervention for tetralogy of Fallot, transposition of the great arteries, and single ventricle heart disease. *J Cardiovasc Comput Tomogr* 2013;7:338-353
33. Goo HW. Initial experience of dual-energy lung perfusion CT using a dual-source CT system in children. *Pediatr Radiol* 2010;40:1536-1544
34. Goo HW. Dual-energy lung perfusion and ventilation CT in children. *Pediatr Radiol* 2013;43:298-307
35. Bauer RW, Kramer S, Renker M, Schell B, Larson MC, Beeres M, et al. Dose and image quality at CT pulmonary angiography-comparison of first and second generation dual-energy CT and 64-slice CT. *Eur Radiol* 2011;21:2139-2147
36. Tang CX, Zhang LJ, Han ZH, Zhou CS, Krazinski AW, Silverman JR, et al. Dual-energy CT based vascular iodine analysis improves sensitivity for peripheral pulmonary artery thrombus detection: an experimental study in canines. *Eur J Radiol* 2013;82:2270-2278
37. Wittram C, Maher MM, Halpern EF, Shepard JA. Attenuation of acute and chronic pulmonary emboli. *Radiology* 2005;235:1050-1054
38. Wittram C, Kalra MK, Maher MM, Greenfield A, McLoud TC, Shepard JA. Acute and chronic pulmonary emboli: angiography-CT correlation. *AJR Am J Roentgenol* 2006;186(6 Suppl 2):S421-S429
39. Thieme SF, Becker CR, Hacker M, Nikolaou K, Reiser MF, Johnson TR. Dual energy CT for the assessment of lung perfusion--correlation to scintigraphy. *Eur J Radiol* 2008;68:369-374
40. Thieme SF, Graute V, Nikolaou K, Maxien D, Reiser MF, Hacker M, et al. Dual Energy CT lung perfusion imaging--correlation with SPECT/CT. *Eur J Radiol* 2012;81:360-365
41. Zhang LJ, Lu L, Bi J, Jin LX, Chai X, Zhao YE, et al. Detection of pulmonary embolism comparison between dual energy CT and MR angiography in a rabbit model. *Acad Radiol* 2010;17:1550-1559
42. Zhang LJ, Zhao YE, Wu SY, Yeh BM, Zhou CS, Hu XB, et al. Pulmonary embolism detection with dual-energy CT: experimental study of dual-source CT in rabbits. *Radiology* 2009;252:61-70
43. Thacker PG, Lee EY. Pulmonary embolism in children. *AJR Am J Roentgenol* 2015;204:1278-1288